Electronic Supplementary Material (ESI) for CrystEngComm.

Intermolecular Interactions and Solubility Behavior of Multicomponent Crystal Forms of 2,4-dichlorophenoxyacetic acid: Design, Structure Analysis, and Solid-State Characterization

Lan Fang[a], Yuntian Xiao[a], Chengtian Zhang[b], Zhenguo Gao[a] *, Songgu Wu [a], Junbo Gong[a, c] *, Sohrab Rohani[d]

[a]School of Chemical Engineering and Technology, State Key Laboratory of Chemical Engineering, Tianjin University; The Co-Innovation Center of Chemistry and Chemical Engineering of Tianjin, Tianjin, 300072, P. R. China

[b]China Nuclear Mining Science and Technology Corporation, Tongzhou, Beijing, 10000, P. R. China

[c]Chemistry and Chemical Engineering Guangdong Laboratory, Shantou 515031, P. R. China

[d]Department of Chemical and Biochemical Engineering, The University of Western Ontario, London, Ontario N6A 5B9, Canada

Contents

Table S1. The salt or cocrystal formers used in failed experiments.
Table S2. Hydrogen bond geometrical parameters of multicomponent crystals
Table S3. The p*K*a and Δp*K*a values of 2,4-D and the coformers
Table S4. HPLC-UV method parameters for 2,4-D
Table S5. HPLC-UV method parameters for IMZ
Table S6. HPLC-UV method parameters for AAP
Table S7. HPLC-UV method parameters for BAP
Table S8. HPLC-UV method parameters for ISO
Table S9. HPLC-UV method parameters for PYM
Table S10. Equilibrium solubility of the 2,4-D concentration of the pure 2,4-D and the 2,4-D multicomponent crystal forms at 25 ℃.
Table S11. Summary Tables of significance analysis of solubility Values
Table S12. The concentration of the 2,4-D and CCF in the 2,4-D multicomponent crystal forms after stability experiments calculated by HPLC
Figure S1. PXRD patterns of the 2,4-D, IMZ, and $(2,4\text{-D})^{+}(\text{IMZ})^{-}$ multicomponent crystals as well as the corresponding simulated patterns of single crystals.
Figure S2. PXRD patterns of the 2,4-D, AAP, and $(2,4\text{-D})^{+}(\text{AAP})^{-}$ multicomponent crystals as well as the corresponding simulated patterns of single crystals.
Figure S3. PXRD patterns of the 2,4-D, BAP, and $(2,4\text{-D})^{+}(\text{BAP})^{-}$ multicomponent crystals as well as the corresponding simulated patterns of single crystals.
Figure S4. PXRD patterns of the 2,4-D, PYM, and 2,4-D-PYM multicomponent crystals as well as the corresponding simulated patterns of single crystals.
Figure S5. PXRD patterns of the 2,4-D, ISO, and 2,4-D-ISO multicomponent crystals as well as the corresponding simulated patterns of single crystals.
Figure S6. Packing similarity matrix of 2,4-D (2), $(2,4\text{-D})^{+}(\text{AAP})^{-}$ (0), and $(2,4\text{-D})^{+}(\text{BAP})^{-}$ (1) calculated by CrystalCMP.
Figure S7. Hirshfeld 2D fingerprints plots of 2,4-D and 2,4-D Multicomponent Crystals.
Figure S8. TG and DSC curves of 2,4-D multicomponent crystals.
Figure S9. PXRD patterns of 2,4-D multicomponent crystals under accelerated storage conditions (40 °C, 75% RH) over 12 weeks. (a)2,4-D, (b) $(2,4\text{-D})^{+}(\text{IMZ})^{-}$, (c) $(2,4\text{-D})^{+}(\text{AAP})^{-}$, (d) $(2,4\text{-D})^{+}(\text{BAP})^{-}$, (e) 2,4-D-ISO and (f) 2,4-D-PYM
Figure S10. DSC patterns of 2,4-D multicomponent crystals under accelerated storage conditions (40 °C, 75% RH) over 3 months.
Figure S11. Standard curve of 2,4-D content (peak area - concentration) determined by HPLC-UV.
Figure S12. Standard curve of IMZ content (peak area - concentration) determined by HPLC-UV.
Figure S13. Standard curve of AAP content (peak area - concentration) determined by HPLC-UV.
Figure S14. Standard curve of BAP content (peak area - concentration) determined by

HPLC-UV.

Figure S15. Standard curve of ISO content (peak area - concentration) determined by HPLC-UV.

Figure S16. Standard curve of PYM content (peak area - concentration) determined by HPLC-UV.

Figure S17. PXRD patterns of 2,4-D and 2,4-D multicomponent crystals before (red line) and after (black line) equilibrium solubility test.

Table S1. The salt or cocrystal formers used in failed experiments.

Compound name	p*K*a (acid)
Nicotinic acid	2.79
Urea	0.18
isoniazid	13.61
Theobromine	9.24
4-Picolinic acid	3.73
Nicotinic hydrazide	13.28

Table S2. Hydrogen bond geometrical parameters of multicomponent crystals

Compound	D–H···A	*d*(H···D) /Å	*d*(H···A) /Å	*θ*(D–H···A) /°	d(D···A) /Å	symmetry code
$(2,4\text{-D})^{+}(IMZ)^{-}$	C_2-H_2···O_2	0.950	2.330	174.18	3.276	-x+1, -y+1, -z+1
	C_7-H_{7B}···O_3	0.990	2.360	170.90	3.341	x-1, y, z
	N_1-H_1···O_3	0.880	1.738	173.34	2.614	
	N_2-H_{2A}···O_2	0.880	1.831	172.24	2.705	-x+1, y-1/2, -z+1/2
	N_2-H_{2A}···O_3	0.880	2.589	130.32	3.228	-x+1, y-1/2, -z+1/2
	C_9-H_9···Cl_2	0.950	2.818	142.68	3.620	x+1, y, z
	C_9-H_9···O_1	0.950	2.625	153.02	3.499	x+1, y, z
$(2,4\text{-D})^{+}(AAP)^{-}$	C_6-H_6···Cl_2	0.950	2.925	146.93	3.757	-x, -y+1, -z+1
	C_7-H_{7B}···O_2	0.990	2.583	171.56	3.565	x, y-1, z
	N_1-H_{1A}···O_3	0.880	1.951	174.59	2.828	
	N_1-H_{1B}···O_3	0.880	2.005	158.23	2.841	-x+3/2, y+1/2, -z+3/2
	N_2-H_{2A}···O_2	0.880	1.862	167.54	2.728	
	C_{12}-H_{12}···Cl_2	0.950	2.962	124.08	3.582	-x+1/2, y+3/2, -z+3/2
	C_{13}-H_{13}···O_2	0.950	2.294	161.05	3.208	-x+1/2, y+1/2, -z+3/2
$(2,4\text{-D})^{+}(BAP)^{-}$	C_2-H_2···Cl_1	0.950	2.892	139.84	3.670	-x+1, -y+1, -z+1
	C_4-H_4···Cl_2	0.950	2.952	162.29	3.868	-x, -y, -z+1
	C_7-H_{7B}···Cl_2	0.990	2.950	173.14	3.935	-x, -y+1, -z+1
	N_1-H_1···O_3	0.923	1.731	176.92	2.653	
	N_2-H_{2A}···O_2	0.864	2.081	160.22	2.909	x+1, y, z
	N_2-H_{2B}···O_2	0.864	2.081	160.22	2.909	-x+1/2, y+1/2, -z+1/2
	C_9-H_9···Cl_1	0.950	2.841	124.62	3.470	x, y-1, z
	C_9-H_9···O_1	0.950	2.653	168.17	3.588	x, y-1, z
	C_{10}-H_{10}···Cl_1	0.950	2.891	123.15	3.502	x, y-1, z
	C_{10}-H_{10}···Cl_2	0.950	2.978	149.09	3.824	-x+1, -y, -z+1
	C_{13}-H_{13}···O_3	0.950	2.262	163.21	3.183	-x+1/2, y+1/2, -z+1/2
2,4-D-PYM	O_3-H_3···O_1	0.820	1.758	169.07	2.568	
	N_1-H_{1A}···O_2	0.860	2.122	158.66	2.940	
	C_{13}-H_{13}···O_3	0.930	2.562	164.03	3.465	-x+2, -y+1, -z+1
	C_4-H_4···O_2	0.930	2.655	138.97	3.411	x-1/2, -y+3/2, z+1/2
2,4-D-ISO	O_3-H_3···N_1	0.840	1.760	176.39	2.599	
	C_7-H_{7A}···O_4	0.990	2.361	144.99	3.222	x-1, y+1, z
	C_7-H_{7B}···O_3	0.990	2.627	134.53	3.395	x-1, y, z
	N_2-H_{2A}···O_4	0.880	2.017	175.76	2.896	-x+3, -y, -z
	N_2-H_{2B}···O_2	0.880	2.089	163.53	2.943	-x+1, -y+1, -z
	C_{12}-H_{12}···O_2	0.950	2.425	162.67	3.344	-x+1, -y+1, -z
	C_{13}-H_{13}···O_2	0.950	2.525	128.09	3.200	

Table S3. The p*K*a and Δp*K*a Values of 2,4-D and the Coformers

p*K*a (pK_{a_1})	coformer	p*K*a (pK_{a_2})	Δp*K*a (pK_{a_2} – pK_{a_1})	forms
2,4-D:2.64	IMZ	6.97	4.33	salt
	AAP	6.84	4.20	salt
	BAP	5.75	3.11	salt
	ISO	3.45	0.81	cocrystal
	PYM	0.5	-2.14	cocrystal

Table S4. HPLC-UV method parameters for 2,4-D

Parameter	Details
Column	C18 column (6 μm, 4.6 mm × 250 mm)
Mobile phase	Phosphoric acid-Buffered aqueous solution-acetonitrile(1:59:40) Buffered aqueous solution contains 0.02 mol/L Sodium dodecyl sulfate SDS and 0.017 mol/L Potassium dihydrogen phosphate.
Flow rate	1 ml/min
Inject volume	20 μL
Column temperature	30 °C
Sample temperature	30 °C
λ_{max}	284 nm
Retention time	5.3 min
Equation	y=4.47414E-7x-0.0075
Regression coefficient(R^2)	0.9998
Calibration range	0.06-4 mg/ml

Table S5. HPLC-UV method parameters for IMZ

Parameter	Details
Column	C18 column (6 μm, 4.6 mm × 250 mm)
Mobile phase	Phosphoric acid-Buffered aqueous solution-acetonitrile(1:59:40) Buffered aqueous solution contains 0.02 mol/L Sodium dodecyl sulfate SDS and 0.017 mol/L Potassium dihydrogen phosphate.
Flow rate	1 ml/min
Inject volume	10 μL
Column temperature	30 °C
Sample temperature	30 °C
λ_{max}	215 nm
Retention time	3.8 min
Equation	y=3.9152E-8x-0.000206
Regression coefficient(R^2)	0.9999
Calibration range	0.01-0.06 mg/ml

Table S6. HPLC-UV method parameters for AAP

Parameter	Details
Column	C18 column (6 μm, 4.6 mm × 250 mm)
Mobile phase	0.025 mol/L Ammonium Dihydrogen Phosphate aqueous solution-methanol (58:42)
Flow rate	1 ml/min
Inject volume	10 μL
Column temperature	30 °C
Sample temperature	30 °C
λ_{max}	290 nm
Retention time	5.1 min
Equation	y=4.56409E-8x-0.0004568
Regression coefficient(R^2)	0.9997
Calibration range	0.01-0.06 mg/ml

Table S7. HPLC-UV method parameters for BAP

Parameter	Details
Column	C18 column (6 μm, 4.6 mm × 250 mm)
Mobile phase	0.025 mol/L Ammonium Dihydrogen Phosphate aqueous solution-methanol (58:42)
Flow rate	1 ml/min
Inject volume	10 μL
Column temperature	30 °C
Sample temperature	30 °C
λ_{max}	282 nm
Retention time	4.3 min
Equation	y=5.47666E-8x-0.0002127
Regression coefficient(R^2)	0.9998
Calibration range	0.005-0.03 mg/ml

Table S8. HPLC-UV method parameters for ISO

Parameter	Details
Column	C18 column (6 μm, 4.6 mm × 250 mm)
Mobile phase	0.02 mol/L Disodium phosphate aqueous solution-methanol (92:8)
Flow rate	1 ml/min
Inject volume	10 μL
Column temperature	30 °C
Sample temperature	30 °C
λ_{max}	258 nm
Retention time	16.6 min
Equation	y=9.66477E-8x+0.000032
Regression coefficient(R^2)	0.9996
Calibration range	0.01-0.06 mg/ml

Table S9. HPLC-UV method parameters for PYM

Parameter	Details
Column	C18 column (6 μm, 4.6 mm × 250 mm)
Mobile phase	water-methanol (90:10)
Flow rate	1 ml/min
Inject volume	10 μL
Column temperature	30 °C
Sample temperature	30 °C
λ_{max}	268 nm
Retention time	8.9 min
Equation	y=2.83833E-8x-0.000656
Regression coefficient(R^2)	0.9998
Calibration range	0.01-0.06 mg/ml

Table S10. Equilibrium solubility of the 2,4-D concentration of the pure 2,4-D and the 2,4-D multicomponent crystal forms at 25 ℃.

Multicomponent crystals	Equilibrium solubility of the 2,4-D concentration at 25 ℃(mg/ml)		
2,4-D	0.515	0.49	0.53
2,4-D-PYM	0.5752	0.54	0.596
2,4-D-ISO	1.9376	1.8	2.1
$(2,4\text{-D})^+(AAP)^-$	4.3045	4.2465	4.4049
$(2,4\text{-D})^+(BAP)^-$	8.2118	8	8.43
$(2,4\text{-D})^+(IMZ)^-$	35.737	35.5	36

Table S11. Summary Tables of significance analysis of solubility Values

2,4-D-PYM:

Analysis of variance: one-way analysis of variance

SUMMARY

Groups	*Counts*	*Sum*	*Average*	*Variance*
Column 1	3	1.535	0.511667	0.000408
Column 2	3	1.711	0.570333	0.0008

ANOVA

Source of Variation	*SS*	*df*	*MS*	*F*	*P-value*	*F crit*
Between Groups	0.005163	1	0.005163	8.542747	0.043123	7.708647
With Groups	0.002417	4	0.000604			
Total	0.00758	5				

2,4-D-ISO:

Analysis of variance: one-way analysis of variance

SUMMARY

Groups	*Counts*	*Sum*	*Average*	*Variance*
Column 1	1.535	0.511667	0.000408	1.535
Column 2	5.839	1.946333	0.022402	5.839

ANOVA

Source of Variation	*SS*	*df*	*MS*	*F*	*P-value*	*F crit*
Between Groups	3.087403	1	3.087403	270.6982	7.99E-05	7.708647
With Groups	0.045621	4	0.011405			
Total	3.133024	5				

$(2,4\text{-D})^{+}(\text{AAP})^{-}$:

Analysis of variance: one-way analysis of variance

SUMMARY

Groups	*Counts*	*Sum*	*Average*	*Variance*
Column 1	3	1.535	0.511667	0.000408
Column 2	3	12.957	4.319	0.006388

Source of Variation	*SS*	*df*	*MS*	*F*	*P-value*	*F crit*
Between Groups	21.74368	1	21.74368	6398.65	1.46E-07	7.708647
With Groups	0.013593	4	0.003398			

Total	21.75727	5				

ANOVA

$(2,4\text{-D})^{+}(\text{BAP})^{-}$:

Analysis of variance: one-way analysis of variance

SUMMARY

Groups	*Counts*	*Sum*	*Average*	*Variance*
Column 1	3	1.535	0.511667	0.000408
Column 2	3	24.651	8.217	0.043909

ANOVA

Source of Variation	*SS*	*df*	*MS*	*F*	*P-value*	*F crit*
Between Groups	89.05824	1	89.05824	4019.116	3.71E-07	7.708647
With Groups	0.088635	4	0.022159			
Total	89.14688	5				

$(2,4\text{-D})^{+}(\text{IMZ})^{-}$:

Analysis of variance: one-way analysis of variance

SUMMARY

Groups	*Counts*	*Sum*	*Average*	*Variance*
Column 1	3	1.535	0.511667	0.000408
Column 2	3	107.246	35.74867	0.059964

ANOVA

Source of Variation	*SS*	*df*	*MS*	*F*	*P-value*	*F crit*
Between Groups	1862.469	1	1862.469	61699.09	1.58E-09	7.708647
With Groups	0.120745	4	0.030186			
Total	1862.59	5				

Table S12. The concentration of the 2,4-D and CCF in the 2,4-D multicomponent crystal forms after stability experiments calculated by HPLC

Multicomponent crystals	2,4-D		CCF		Stoichiometric ratio
	peak area	Concentration (mmol/ml)	peak area	Concentration (mmol/ml)	
2,4-D-PYM	232110	4.36 E-4	1912301	4.36 E-4	1:1
2,4-D-ISO	226210	4.24 E-4	534990	4.24 E-4	1:1
$(2,4\text{-D})^{+}(\text{AAP})^{-}$	305749	5.85 E-4	1215010	5.85 E-4	1:1
$(2,4\text{-D})^{+}(\text{BAP})^{-}$	170094	3.10 E-4	536678	3.10 E-4	1:1
$(2,4\text{-D})^{+}(\text{IMZ})^{-}$	451690	8.81 E-4	1534600	8.81 E-4	1:1

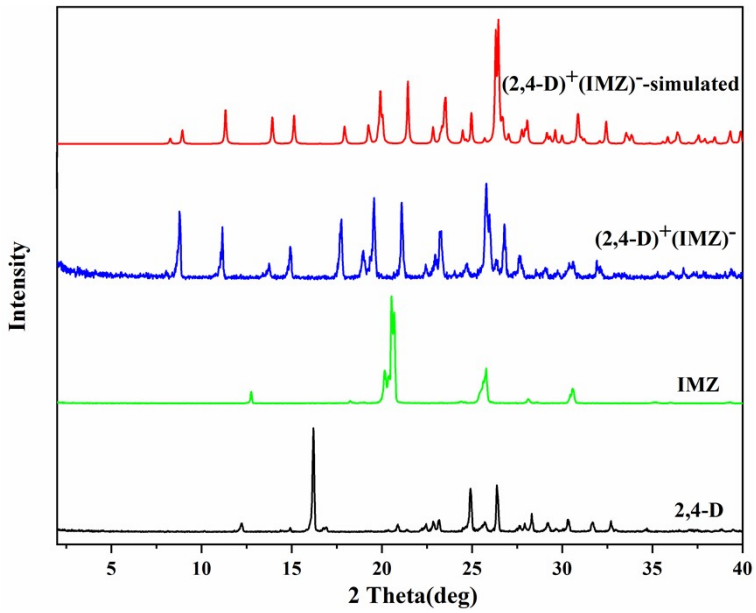

Figure S1. PXRD patterns of the 2,4-D, IMZ, and $(2,4\text{-D})^{+}(\text{IMZ})^{-}$ multicomponent crystals as well as the corresponding simulated patterns of single crystals.

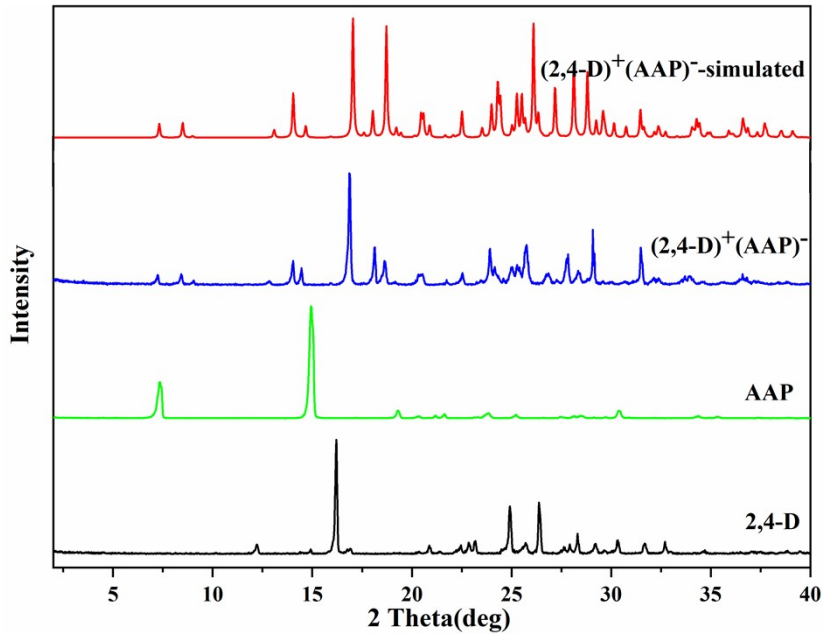

Figure S2. PXRD patterns of the 2,4-D, AAP, and $(2,4\text{-D})^{+}(\text{AAP})^{-}$ multicomponent crystals as well as the corresponding simulated patterns of single crystals.

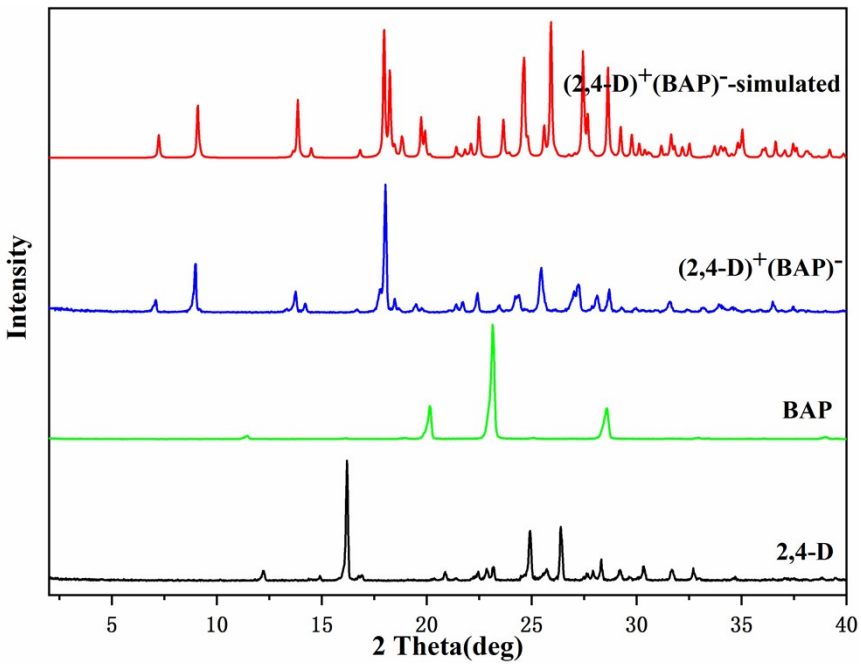

Figure S3. PXRD patterns of the 2,4-D, BAP, and $(2,4\text{-D})^{+}(\text{BAP})^{-}$ multicomponent crystals as well as the corresponding simulated patterns of single crystals.

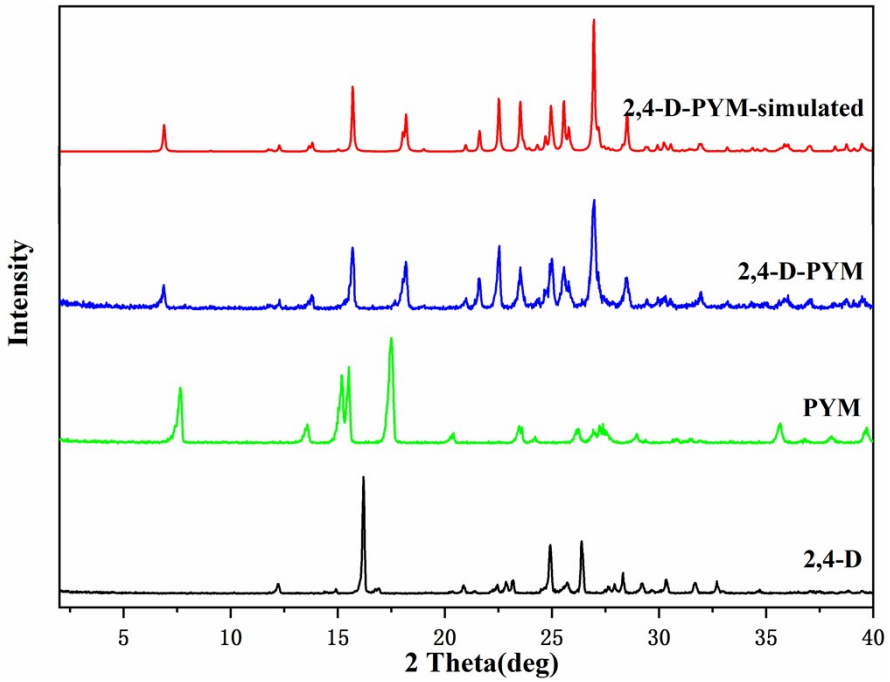

Figure S4. PXRD patterns of the 2,4-D, PYM, and 2,4-D-PYM multicomponent crystals as well as the corresponding simulated patterns of single crystals.

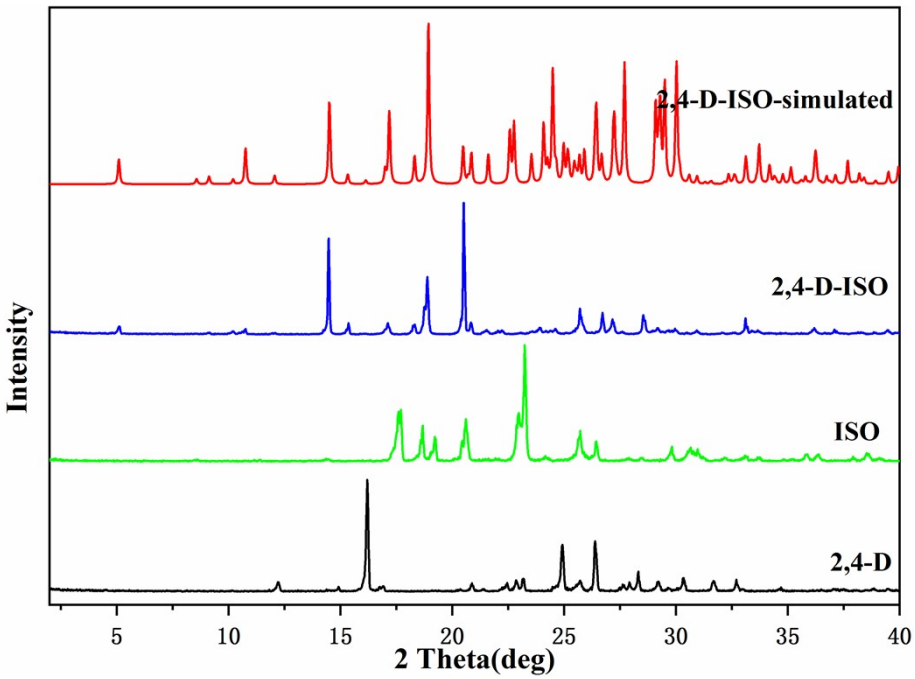

Figure S5. PXRD patterns of the 2,4-D, ISO, and 2,4-D-ISO multicomponent crystals as well as the corresponding simulated patterns of single crystals.

	0	1	2
0	0.000	3.046	205.70
1	3.046	0.000	199.66
2	205.70	199.66	0.000

Figure S6. Packing similarity matrix of 2,4-D (2), $(2,4\text{-D})^{+}(AAP)^{-}$ (0) and $(2,4\text{-D})^{+}(BAP)^{-}$ (1) calculated by CrystalCMP.

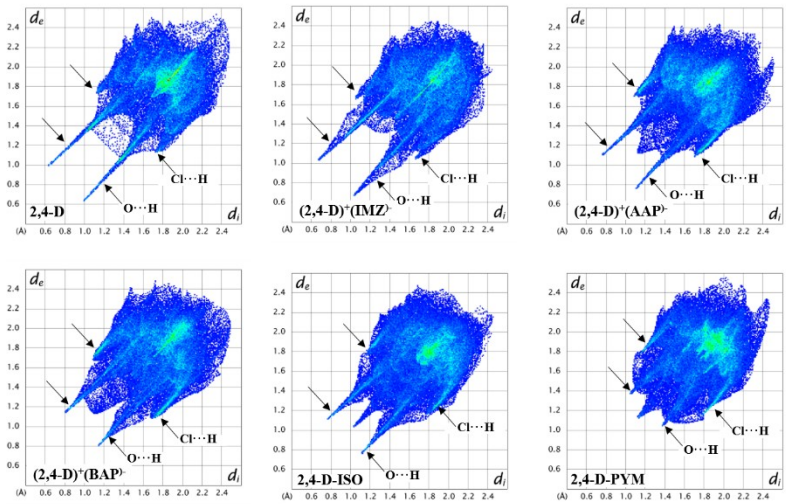

Figure S7. Hirshfeld 2D fingerprints plots of 2,4-D and 2,4-D Multicomponent Crystals.

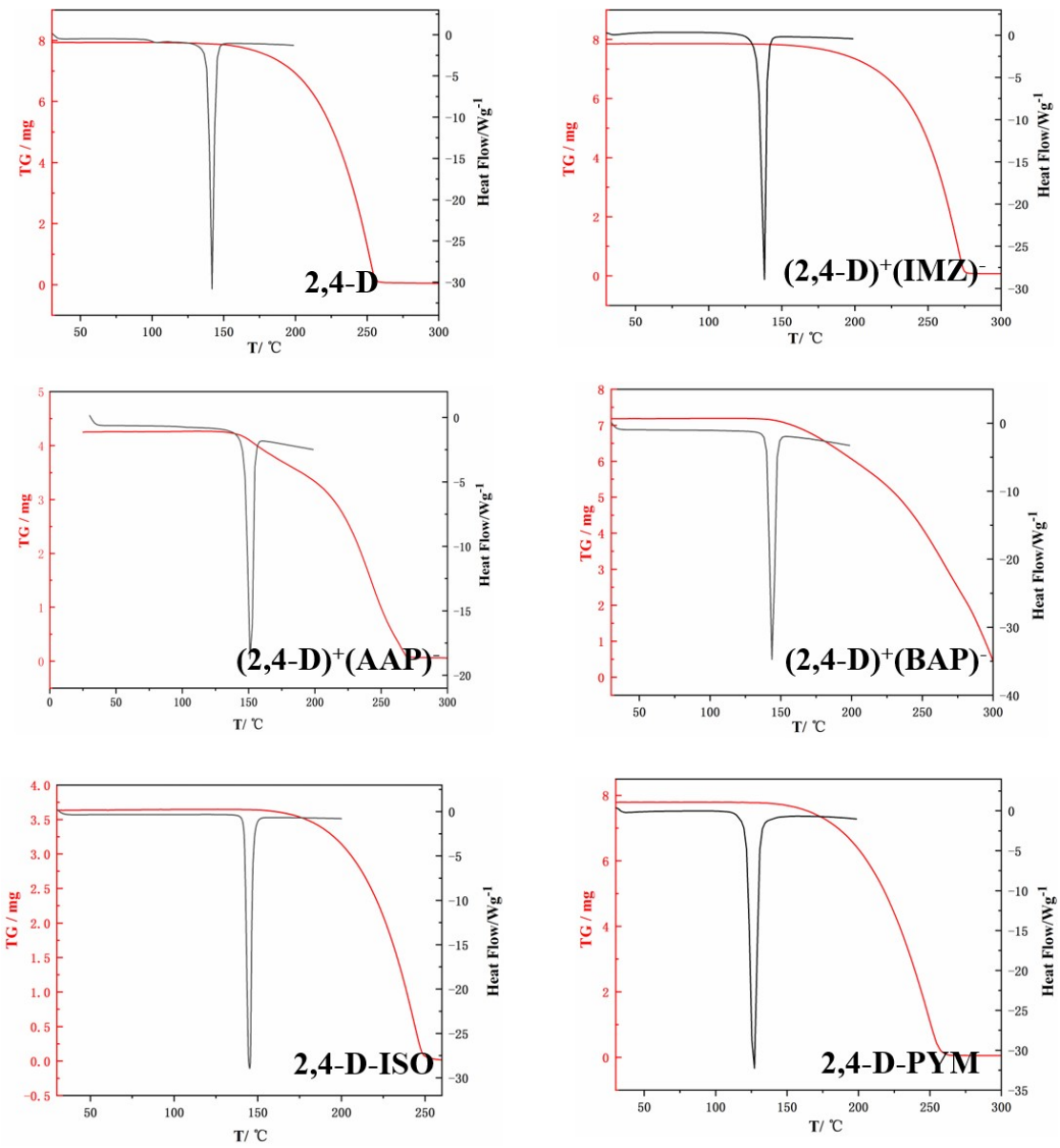

Figure S8. TG and DSC curves of 2,4-D and 2,4-D multicomponent crystals.

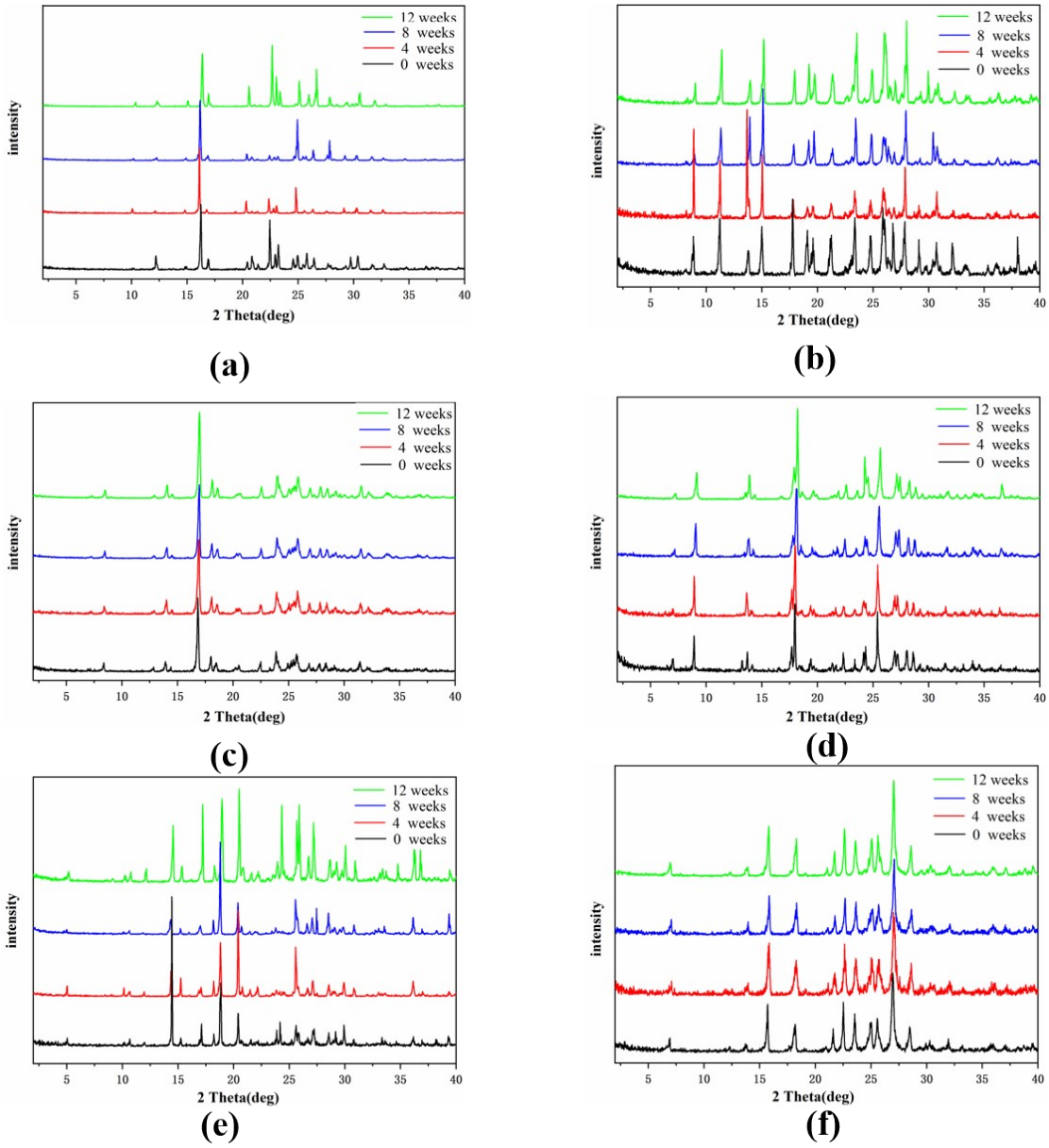

Figure S9. PXRD patterns of 2,4-D multicomponent crystals under accelerated storage conditions (40 °C, 75% RH) over 12 weeks. (a)2,4-D, (b) $(2,4\text{-D})^{+}(\text{IMZ})^{-}$, (c) $(2,4\text{-D})^{+}(\text{AAP})^{-}$, (d) $(2,4\text{-D})^{+}(\text{BAP})^{-}$, (e) 2,4-D-ISO, and (f) 2,4-D-PYM

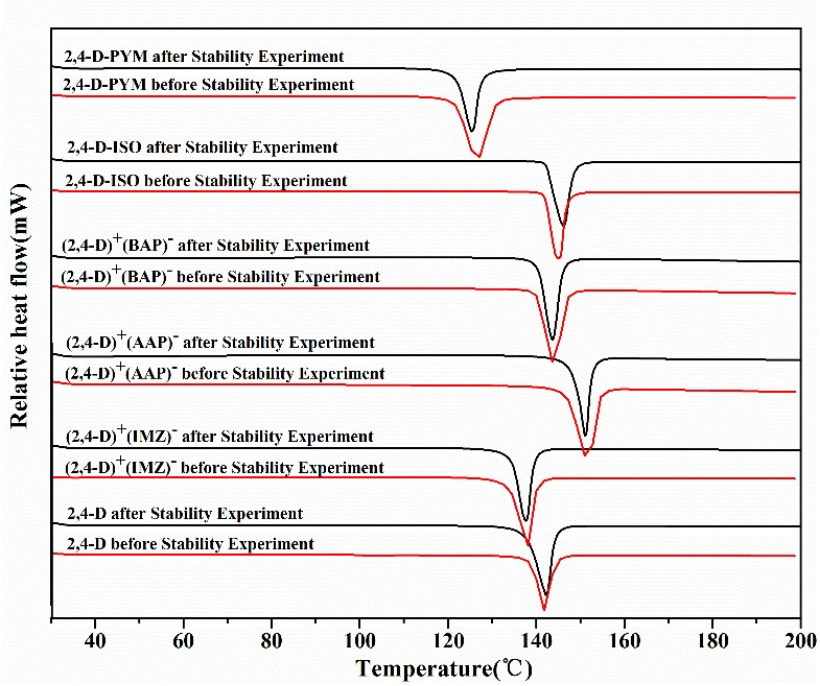

Figure S10. DSC patterns of 2,4-D and 2,4-D multicomponent crystals under accelerated storage conditions (40 °C, 75% RH) over 3 months.

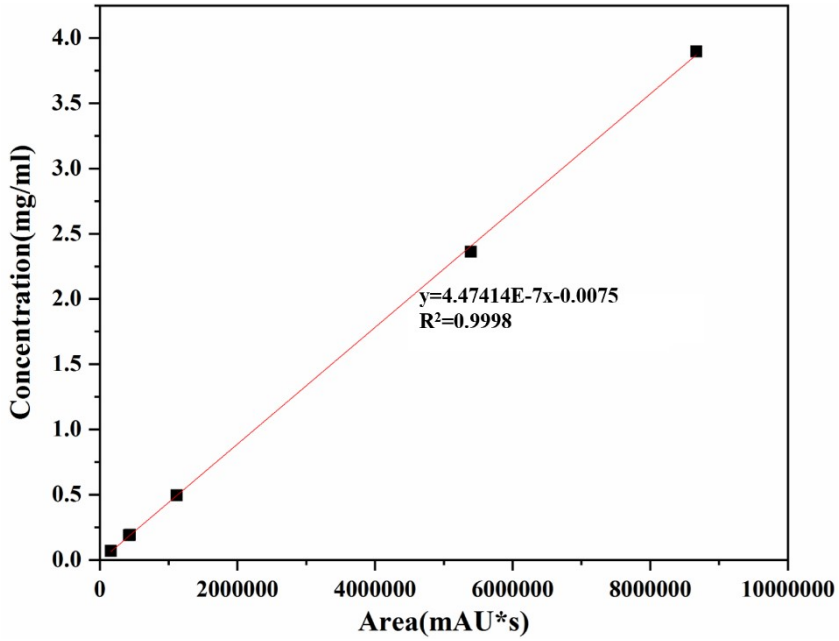

Figure S11. Standard curve of 2,4-D content (peak area - concentration) determined by HPLC-UV.

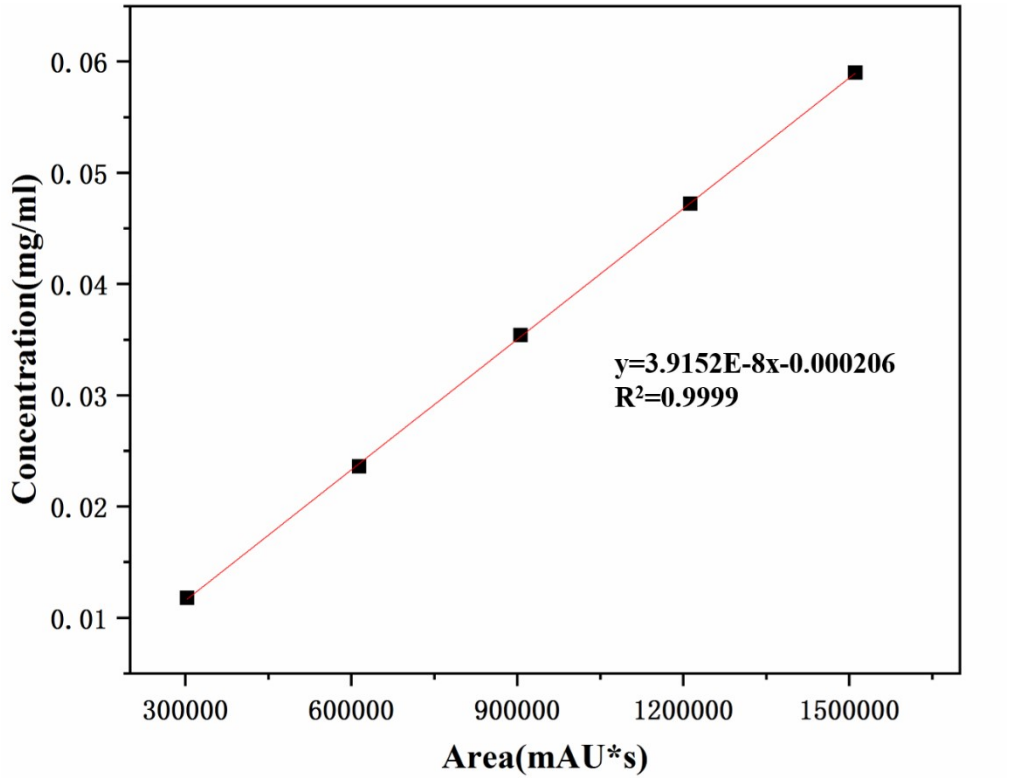

Figure S12. Standard curve of IMZ content (peak area - concentration) determined by HPLC-UV.

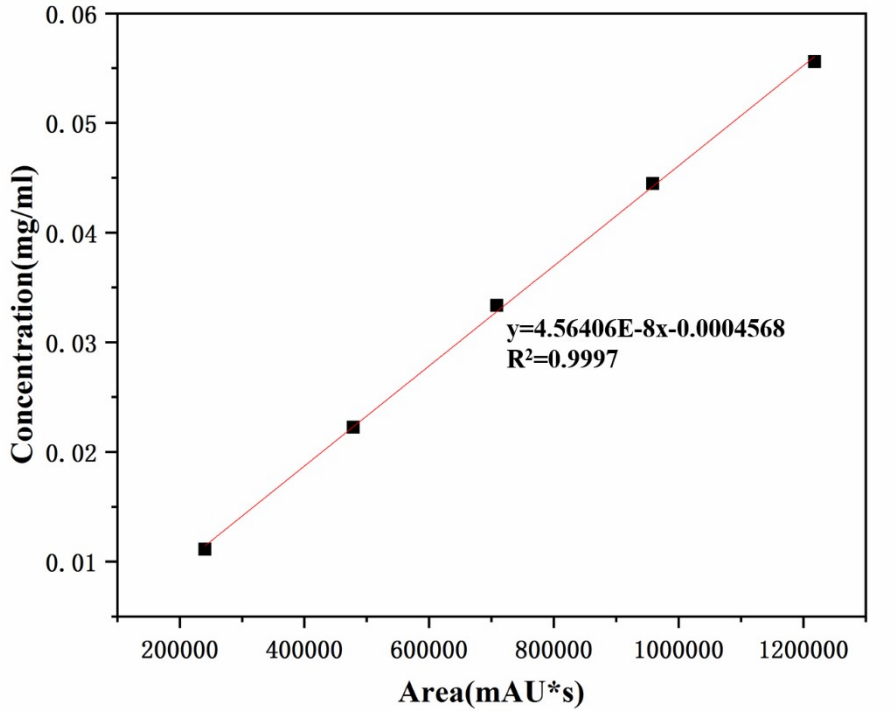

Figure S13. Standard curve of AAP content (peak area - concentration) determined by HPLC-UV.

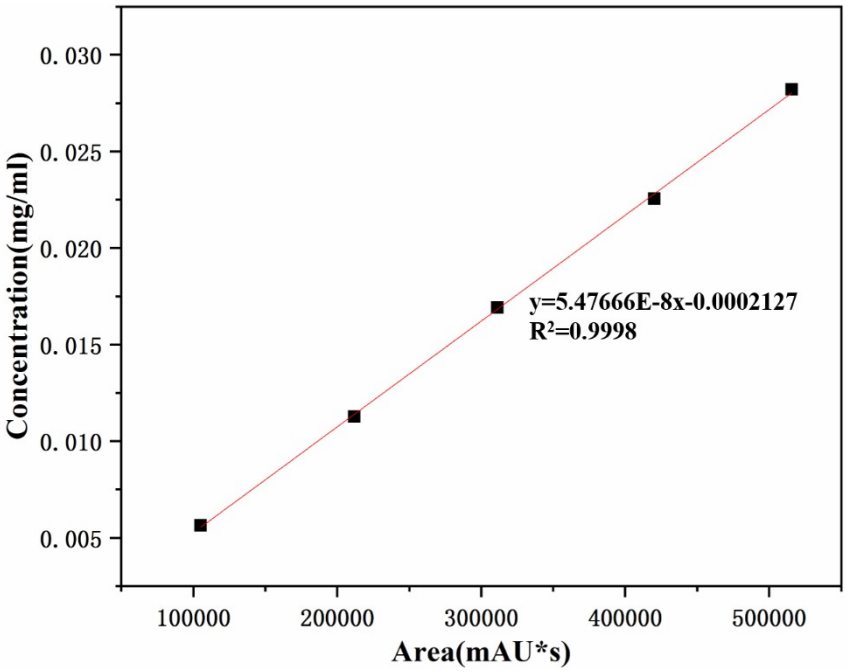

Figure S14. Standard curve of BAP content (peak area - concentration) determined by HPLC-UV.

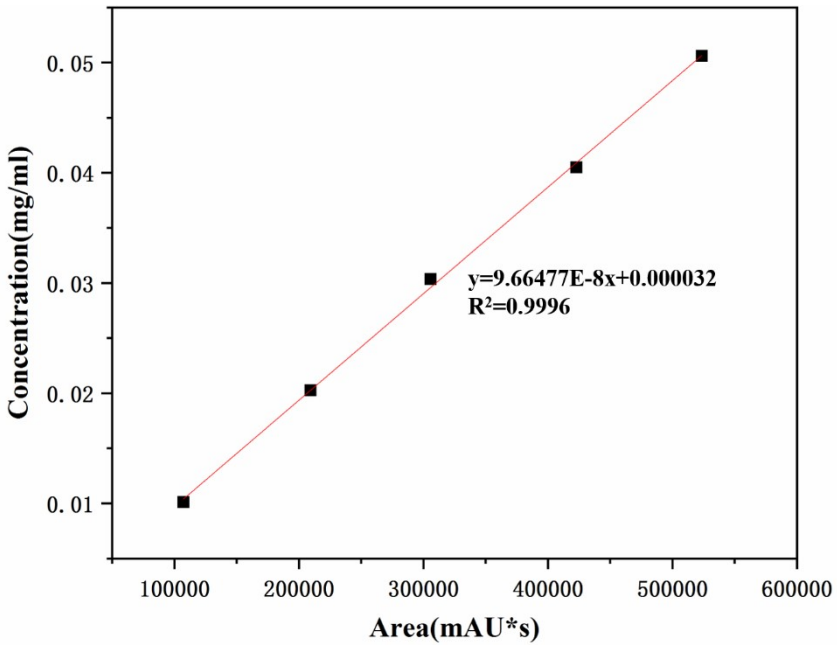

Figure S15. Standard curve of ISO content (peak area - concentration) determined by HPLC-UV.

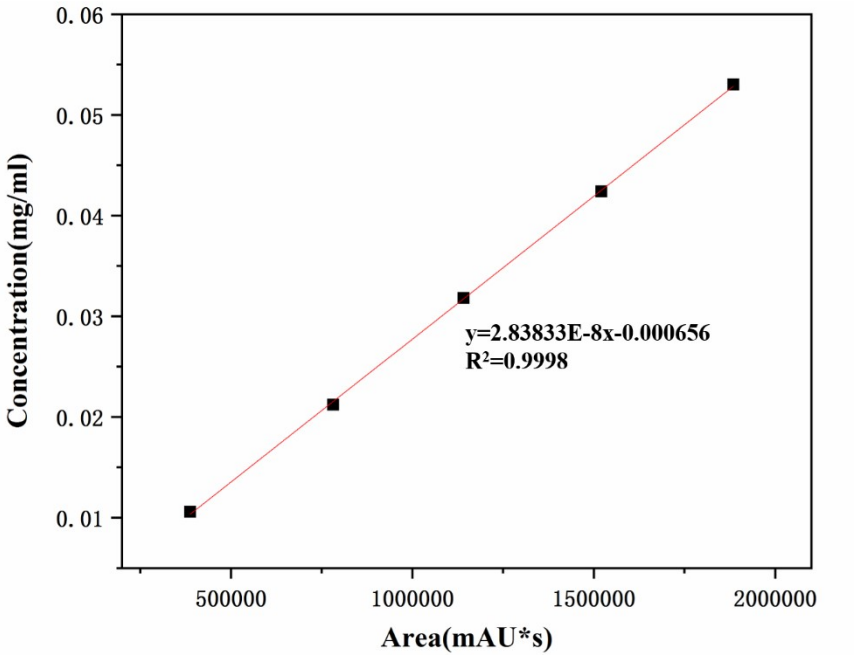

Figure S16. Standard curve of PYM content (peak area - concentration) determined by HPLC-UV.

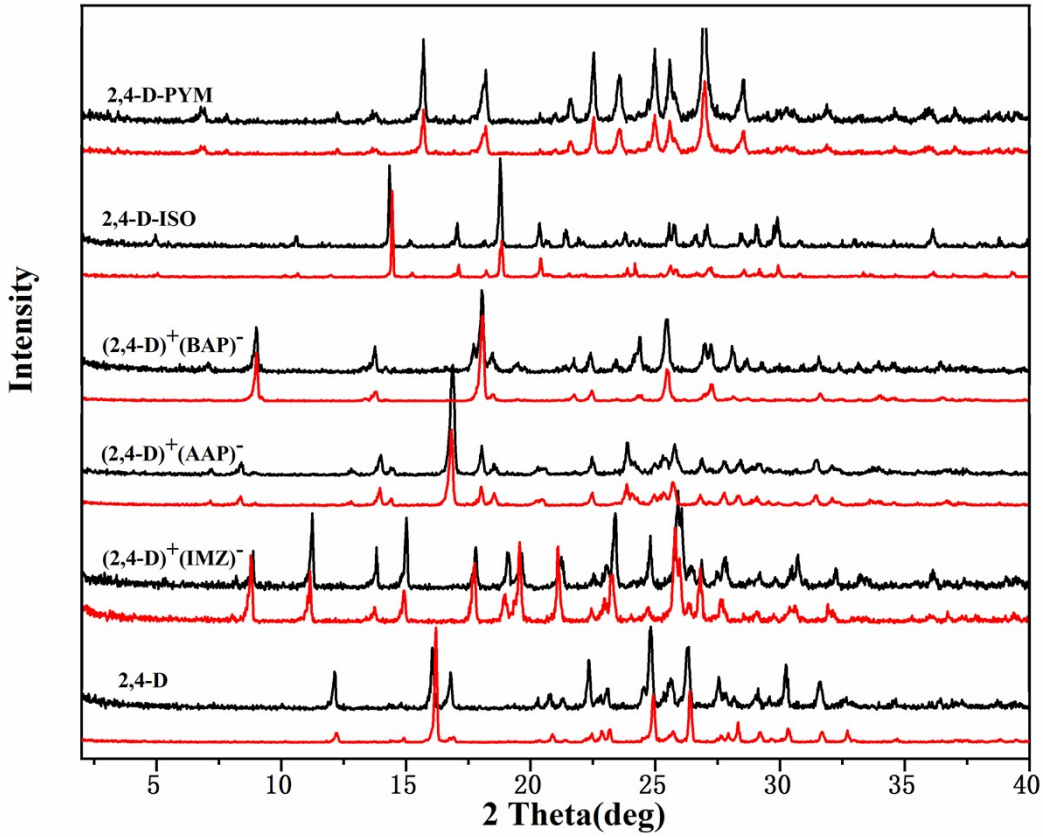

Figure S17. PXRD patterns of 2,4-D and 2,4-D multicomponent crystals before (red line) and after (black line) equilibrium solubility test.